IECO International Journal Of Industrial Electronics Control and Optimization
Print ISSN: 3517-2645
Online ISSN: 3568-2645
Homepage: https://ieco.usb.ac.ir/

# Diagnosis Of Supercapacitor State-Of-Charge In Electric Vehicle Applications Using Artificial Neural Networks

Seyed-Saeid Moosavi-Anchehpoli[1] | Mahmood Moghadasian [2] | Maryam Golpour [3]

[1]Clean power generation and Electrochemical laboratory, Amol University of Special Modern Technologies, IRAN
[2] Shohadaye Hoveizeh Campus of Technology, Shahid Chamran University of Ahvaz, IRAN
[3] Clean power generation and Electrochemical laboratory, Amol University of Special Modern Technologies, IRAN
Corresponding author's email: anchepoli@um.ac.ir

**Article Info**

**Article type:**
Research Article

**Article history:**
Received: **********
Received in revised form: **********
Accepted: **********
Published online: **********

**Keywords**:
State-of-charge,
wavelet transform,
Artificial neural network,
Supercapacitor.

**ABSTRACT**

In electric vehicles, energy storage systems (ESSs) are essential for managing power fluctuations and ensuring operational safety. Supercapacitors (SCs) have recently emerged as promising ESS candidates due to their high-power density, rapid charge/discharge capabilities, and low internal losses. Integrating SCs with batteries or fuel cells in hybrid configurations can leverage the strengths of each technology while mitigating their individual weaknesses. This paper presents a novel estimation technique for supercapacitors in electric vehicles. The method involves wavelet decomposition and denoising, followed by importing low-frequency signals into a back-propagation neural network for one-step prediction to determine the state-of-charge (SOC) of the SC. The proposed method is tested with a Maxwell supercapacitor model under various charge/discharge current profiles and temperature conditions, comparing the results with conventional techniques. The artificial neural networks (ANNs) with wavelet pre-processed input demonstrate significantly improved SOC estimation accuracy across different discharge profiles.

## I. Introduction

Batteries like Li-ion offer high energy density for electric vehicles, but their limited lifespan and sensitivity to charging rates and temperature present significant challenges. Combining them with supercapacitors (SCs) in a hybrid energy storage system (HESS) is a promising solution to enhance efficiency and address these limitations, as research has shown [1]. Accurately diagnosing the state-of-charge (SOC) of supercapacitors is vital for managing energy distribution between the supercapacitor and the battery, optimizing performance, and ensuring the reliability of EVs [2].

The SOC of a supercapacitor, indicating its remaining energy relative to its maximum capacity, is crucial for effective energy management, ensuring the supercapacitor operates within safe limits, and optimizing the performance and lifespan of the entire energy storage system [3].

Estimating the State of Charge of a supercapacitor, is crucial for efficient and safe operation. However, traditional methods often struggle with the inherent nonlinearities and dynamic characteristics of these devices. These methods fall into several categories:

Direct Measurement Methods: These methods rely on directly measurable parameters of the energy storage device.

Coulomb Counting: Coulomb counting is a straightforward method that integrates the current over time. While simple, this method suffers from cumulative error over time and requires an accurate initial SOC value [4].

Voltage-based: These methods estimate SOC by measuring the terminal voltage of the supercapacitor. However, the nonlinear relationship between voltage and SOC, particularly at high and low extremes, limits accuracy [5].

Current Integration: SOC is estimated by integrating the current flowing in or out of the device over time. This method suffers from drift and requires accurate initial SOC [6].

Model-Based Methods: These methods utilize mathematical models of the energy storage device.

Equivalent Circuit Models: Represent the device with electrical components (resistors, capacitors, inductors) to simulate behavior and estimate SOC. Accuracy depends on model complexity and parameter identification [18].

Electrochemical Models: More complex models based on the underlying electrochemical reactions within the device, offer higher accuracy but require significant computational resources [7].

Kalman Filtering: A recursive algorithm that combines model predictions with measurements to estimate SOC, reducing noise and improving accuracy. Requires a well-defined model and can be computationally demanding [1].

Data-Driven Methods: These methods leverage machine learning algorithms trained on historical or experimental data.

Artificial Neural Networks: ANNs have shown promise in SOC estimation due to their ability to capture complex, nonlinear relationships without explicit mathematical models. ANNs can learn from historical data and adapt to new conditions, making them suitable for dynamic environments like EVs [8-10].

Support Vector Machines: Effective for classification and regression tasks, can be used for SOC estimation. Require careful selection of kernel functions and hyperparameters [11].

Fuzzy Logic: Handles uncertainties and non-linearities well, suitable for complex systems. Requires expert knowledge for rule definition and membership function design [12].

Hybrid Methods: Combine multiple approaches to leverage their strengths and mitigate weaknesses. For example, combining an ECM with a Kalman filter or using an ANN to improve the accuracy of a voltage-based method [13].

This categorization is not exhaustive, and new methods are constantly being developed. The choice of the most suitable method depends on factors like the specific energy storage device, required accuracy, computational resources, and application requirements.

Modeling the behavior of supercapacitors is challenging due to their complex dependence on current, temperature, chemistry, and past conditions [8]. Traditional methods struggle with such intricate nonlinearities. Artificial Neural Networks (ANNs) offer a powerful alternative, excelling at capturing complex relationships without requiring explicit mathematical equations or physical derivations.

When tackling a nonlinear system like a supercapacitor, ANNs bypass the need for cumbersome calculations. Instead, they learn by analyzing a carefully chosen data set. By adjusting internal connections (neurons) and iteratively fine-tuning them, the ANN gradually approximates the system's behavior. Remarkably, even with limited data, ANNs can identify subtle patterns and adapt to unseen situations.

A well-trained ANN exhibits resilience to unexpected inputs, including noise and disruptions. This robustness allows it to deliver accurate predictions even in uncertain environments [9, 10].

In contrast to the aforementioned approaches, ANNs have emerged as a popular tool for estimating SOC in both batteries and supercapacitors, handling both constant and dynamic discharge currents [8, 10]. Several variables are chosen as the ANN's inputs. The weights are usually trained using a BP algorithm. Reported error margins vary, with references claiming accuracy within 10% [8]. However, recent breakthroughs have led to significantly improved accuracy, with some researchers reporting error rates as low as 1% [14-19].

For modeling supercapacitors in automotive applications, research suggests using a one-layer feed-forward ANN trained with the back-propagation algorithm [8]. Similarly, an ANN-based performance computing model for lead-acid batteries in EVs has been proposed in [10].

These neural network approaches exhibit greater accuracy compared to traditional methods like the Peukert equation (maximum error 1.724%), multilevel Peukert equation (maximum error 1.379%), and least-square method (maximum error 1.379%). Studies show that the proposed ANN models achieve significantly lower errors [8].

For energy management and optimal power control, establishing a precise model to display SC dynamics behavior is critical; however, this is difficult.

The following are the key contributions of this work:

1- To improve the conventional function of training ANN, a WT model is created. It's used to break down a voltage profile into its various components, each with its own frequency.

2- The number of neurons in multi-layer neural networks is optimized.

3- The proposed WT model and ANN’s are combined to create a complete wavelet ANN model, which greatly improves SOC estimation accuracy.

4- The proposed wavelet ANN model exhibited robust performance across a range of driving cycles (discharge current profiles), consistently providing reliable SOC estimations with low error rates. These results compare favorably to those reported in the literature.

5- The classification unit is not needed for categorizing the different discharge current profiles in this ANN system. This is yet another significant outcome of this project.

6- The given technique can be employed to precisely determine the SOC of a SCs module, which is exceptionally beneficial in EV applications.

The layout of this study is as follows: Section 2 covers the background on WT. Section 3 delves into the background of ANN. Section 4 outlines the details of the test bench. The outcomes and relevant discussions are unveiled in Section 5. Lastly, the conclusion of this study is drawn in Section 6.

## II. Wavelet Transform (WT) Specification

Given that the Fourier transform (FT) fails to pinpoint the exact moment of a specific frequency's appearance within a signal time series, it proves inadequate for examining nonstationary signals. Conversely, the wavelet transform (WT) transposes a signal from the time domain (TD) into a time-scaled frequency domain (TSFD). This method enables a nonstationary and nonlinear signal profile to be disassembled into a set of profiles, each with distinct frequencies. Wavelet [20] is a short-duration wave that develops and decays over a short period of time.

The Wavelet Transform (WT) breaks down a signal into its building blocks based on frequency. It separates the signal into two types of information:

Approximation (A) data: This captures the overall trend and low-frequency components of the signal. Think of it like the smooth outline of a painting.

Detail (D) data: This contains the high-frequency details and sharp features, like the brushstrokes and textures in the painting.

However, unlike traditional WT, which only analyzes the low-frequency part, the method used here goes further. It decomposes the signal into multiple levels (like zooming in on the painting). This allows for a more detailed understanding of both the overall shape and the fine details.

Figure 1 illustrates this three-level decomposition. In the notation Aα; β and Dα; β, α represents the level (zoom level) and β is an index that identifies specific signals within that level.

Various stages of decomposition can be undertaken, but studies indicate that the tri-level decomposition exhibits superior performance in other time series prediction applications, such as power system load forecasting in the conventional wavelet transformation [21]. WT bifurcates into two classifications: the Continuous Wavelet Transform (CWT) and the Discrete Wavelet Transform (DWT). The CWT encapsulates all the information contained in the provided signal x(t), as represented by Eq. (1).

$$W(a,b) = \int_{-\infty}^{\infty} \psi_{a,b}(t) \cdot x(t) dt \tag{1}$$

CWT, on the other hand, is computationally inefficient and needs a lot of memory compared to DWT. DWT is accurate enough to decompose a signal while still being computationally light. As a result, we use a DWT in this analysis. For a particular signal, denoted as x(t), the definition of DWT is expressed in Eq. (2).

$$W(m,n) = 2^{-(m/2)} \sum_{t=0}^{T} \psi\left(\frac{t - n \cdot 2^m}{2^m}\right) \cdot x(t) \tag{2}$$

In this context, T denotes the duration of the signal x(t), with m and n symbolizing the scaling and translational parameters in such a manner that ($a = 2^m$) and ($b = n \cdot 2^m$). Further, t represents the individual time parameter in its discrete form.

## III. ANN Model Specification

The artificial neural network has long been recognized as an effective estimation method for both linear and non-linear systems. ANNs can be used to model nonlinear dynamic systems to some level of precision [22].

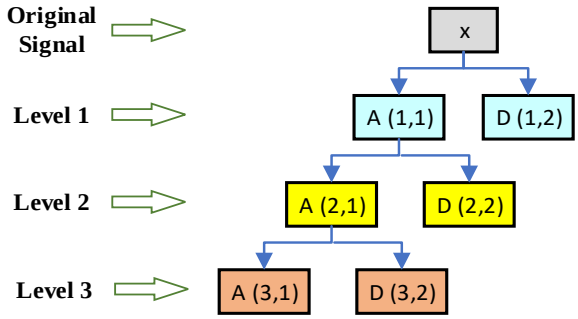


Fig. 1. A WT with Three-level. In both A (α, β) and D (α, β), α is symbolic of the levels, whereas β indicates the position of the signal within the level noted by α.

ANNs offer a multitude of benefits, comprising the capacity to discern intricate nonlinear links between dependent and independent variables, bypassing the requirement for formal statistical education. Additionally, they can identify every conceivable correlation among predictive variables and provide a plethora of training algorithms [8, 9]. Despite these advantages, they also possess certain drawbacks such as their 'black box' structure, increased computational demand, tendency towards overfitting, and the practical essence of model building [23]. The structure of a ANN outlines the configuration of neural connections, along with the categorization of units characterized by an activation function. The processing algorithm defines the method through which neurons compute the output vector, given a specific set of weights for each input vector. The training algorithm explicates how the ANN modifies its weights 'w' corresponding to all input vectors, also known as training vectors.

As a result of the training algorithm, the ANN will gain information and store it in synaptic weights. There are several different types of ANNs, but multi-layer feed-forward networks are the most common. Figure 2 shows a sample feed-forward ANN scheme (input, one hidden layer, and output layer) [24, 25].

This work employs a three-layers, Feed Forward ANN to estimate the SOC. In the construction of an ANN, neurons function as fundamental components. As illustrated in Figure 3, an ANN's single layer can have 'i' inputs given by X = [x1, x2 … xi]T and 'k' neurons. It should be noted that 'k' is typically not equal to 'i'. Furthermore, each input is linked to individual neurons through suitable weightings.

Every neuron computes the cumulative total of its inputs, factoring in the bias, and subjects this result to its activation function. Consequently, there are 'k' resultant outputs y1= [y11, y12 … y1k]T associated with the ANN represented by a singular layer (where the primary index in y1 outcomes of the first layer is detailed as y11, y12 … y1k) and,

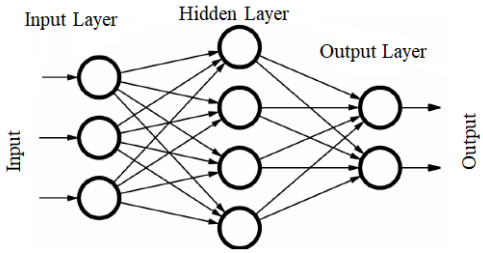


Fig. 2. Sample of a feed-forward ANN

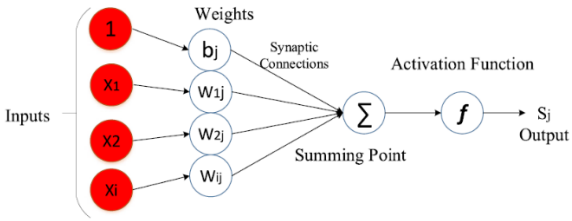


Fig. 3. The diagram of a neuron

$$y_1 = F_1 (W_1X + B_1) \quad (3)$$

The term 'F1' signifies the activation matrix pertaining to this individual layer. This matrix is characterized by being diagonal and consisting of k elements. The matrix's nature is contingent on the net inputs directed towards this specific layer.

$$F1 (S1) = diag [f1s1, f1s1 ... f1(sk)] \quad (4)$$

The elements mentioned are the activation functions for each of the 'k' nodes, which are presumed to be identical, denoted as f11=f12=...=f1k=f1. 'S1' represents the net vector, S1= [s1, s2,..., sk]T, comprising the net inputs s1, s2,..., sk for neurons 1, 2, ..., K, and S_j equals $S_j = \sum_{j=1}^{n} w_{ij} x_j (t) + b_i$. Additionally, '$w_1$' signifies the weight matrix for the output layer, which due to the predefined structure, must encompass k rows and n columns.

$$w_1 = \begin{bmatrix} w_{1,1} & w_{1,2} \cdots & w_{1,n} \\ \vdots & \ddots & \vdots \\ w_{k,1} & w_{k,2} \cdots & w_{k,n} \end{bmatrix} \quad (5)$$

The term '$w_{ij}$' typically represents the weight transitioning from target node 'j' to origin node 'i', given that i and j are any numbers from 1 to k and 1 to n respectively. B1, on the other hand, signifies the bias vector for a single layer, expressed as B1 = [b11, b12, ..., b1k]T. Here, b11, b12, ..., b1k denote the individual biases of nodes ranging from 1 to k in the final layer. We can construct an ANN with three lyres by extending the aforementioned equations. In this study, a mere 10 cycles of SC voltage profiles were utilized as training data and for estimating the state-of-charge.

## IV. Experimental Set-Up

Figure 4 depicts the experimental setup. The trials employed a SC cell provided by Maxwell Technologies, boasting a specified voltage of 2.7 V and a capacitance of 350 F. Comprehensive data regarding the SC cell's parameters can be found in Table I.

TABLE 1 THE SYSTEM'S EXPERIMENTAL PARAMETERS

| Parameter | Value |
|---|---|
| Supercapacitor cell | Maxwell technology |
| Rated voltage of cell | 2.7 V |
| Rated capacitance of cell | 350 F |
| Sampling frequency fs | 50 Hz |
| Operating temperature T °c | 0 , 25, 35, 45 , 55 |
| Minimum Temperature °c | -40 |
| Maximum Temperature °c | 70 |
| Absolute maximum voltage | 2.85 V |
| Absolute maximum Current | 170 A |
| Maximum ESRDC initial | 3.2 m.ohm |
| Specific energy | 5.6 wh/Kg |
| Leakage current (at 25 °c) | 0.3 mA |
| Maximum continuous Current 15°C | 21 A |
| Maximum continuous Current 40°C | 34 A |
| Life time | 500000 life cycle |

The SC's charge and discharge current is monitored and controlled by a battery testing and formulation system, both software and hardware, courtesy of BaSyTec technology. This system is used to generate the required current profiles and to mimic the conditions experienced during real-world Electric Vehicle (EV) driving scenarios. T=25°C, 35°C, 45°C, and 55°C are the temperatures used in the experiments. The Battery test device is limited to a sampling frequency of fs=50 Hz. For data acquisition, eight different current discharge profiles are employed, as follow:

- Worldwide harmonized Light vehicles Test Cycles (WLTC)
- Artemis cycle with maximum speeds of 130 (Art 130)
- Artemis Urban (Art Urban)
- Artemis Rural (Art Rural)
- West Virginia Suburban (WVUSUB) driving cycle
- Japan Cycle 08 (JC08)
- Japan 10-15 mode (JP1015)

- New European Driving Cycle (NEDC)

## V. Results and Discussion

A diagnostic process and implementation algorithm for SOC estimation of SC are shown in Figure 5. The next step is ANN training after identifying a proper pattern with wavelet transform, as shown in figure 6 and outlined in section II. This enables one to gain a better understanding of the ANN mechanism prior to its implementation. The NN's learning algorithm is a computational method that determines the strength of connections, such as layer weights and biases in neurons. The validation data collection is used during the learning process to boost the ANN's generality. The learning process is terminated based on the validation data set when the error function starts to increase or becomes smaller than the convergence tolerance, whichever comes first.

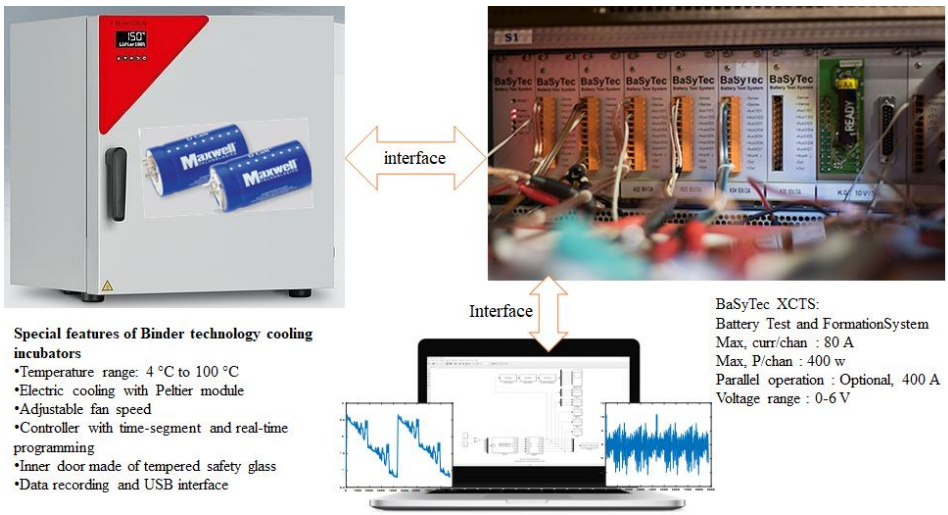


Fig. 4. Pictures of the experimental setup

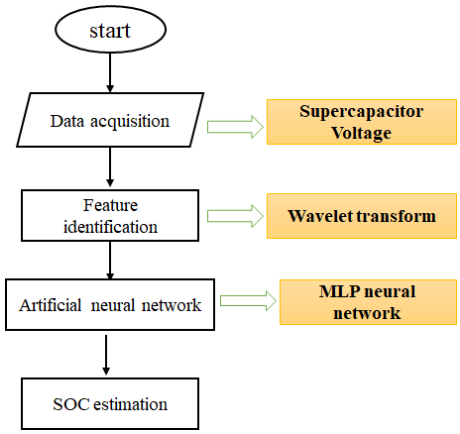


Fig. 5. SOC estimation and implementation algorithm

We use the data to train a neural network, in which, the hidden layer contains 30 neurons. Hyperbolic tangent (Tanh) function is used as an activation function. The maximum number of epochs is set to 100, and validation MSE goal is set to 1e-6. Since the Levenberg–Marquardt algorithm has a fast rate of convergence, we use it to train the parameters of the neural networks in this study. The training performance of the ANN has been shown in figure 7. The best validation MSE is 0.0001318 at epoch 87.

The data are randomly divided into three sets: training (60% of the data), testing (20%), and crossvalidation (20%) as shown in the Table II. All data are normalized in the range of [0, 1].

The accuracy of SOC estimation is analyzed using five established error metrics:

Mean Square Error (MSE), Root Mean Square Error (RMSE), and Normalized Root Mean Square Error (NRMSE): These metrics quantify the average magnitude of errors between predicted and actual SOC values.

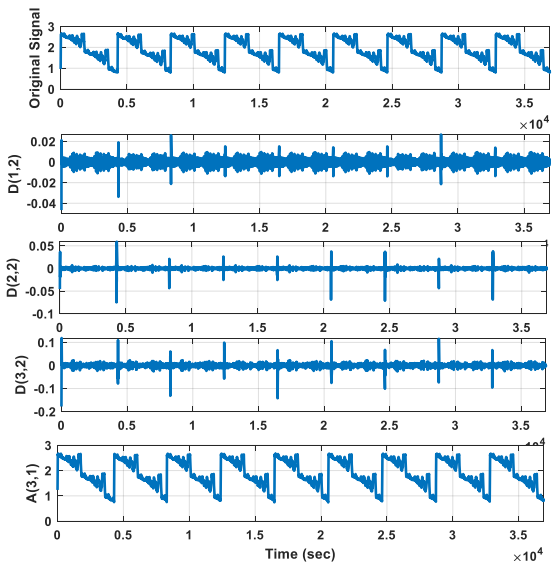

Fig. 6. Output results from a 3-level WT intended for ANN training input, derived solely from a single current discharge profile

NRMSE normalizes the error by the SOC range, allowing for comparisons across different datasets.

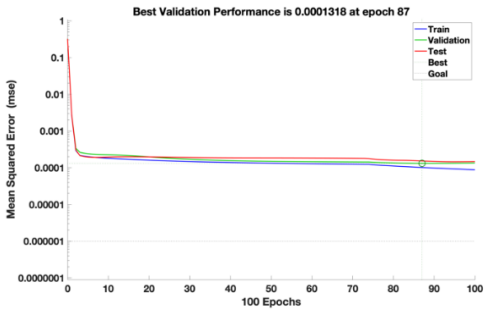


Fig. 7. Training performance of the ANN

TABLE 2 DATA DIVISION IN LEARNING PROCESS

| Discharge Profile | Number of All Data Samples | Number of Training Samples | Number of Testing Samples |
|---|---|---|---|
| WLTC | 40000 | 24000 | 8000 |
| Art 130 | 16250 | 9750 | 3250 |
| Art Urban | 10000 | 6000 | 2000 |
| Art Rural | 2000 | 1200 | 400 |
| WVUSUB | 10000 | 6000 | 2000 |
| JC08 | 8000 | 4800 | 1600 |
| JP1015 | 7500 | 4500 | 1500 |
| NEDC | 10000 | 6000 | 2000 |

Average Relative Percentage Error (ARPE): This metric expresses the average error as a percentage of the actual SOC values, providing a relative measure of accuracy.

By analyzing these error metrics across all three data sets, this work provides a comprehensive understanding of the ANN's generalizability and effectiveness in real-world applications.

$$MSE = \frac{1}{N}\sum_{j=1}^{N}(U_a(j) - U_a(j))^2 \quad (6)$$

$$RMSE = \sqrt{\frac{\sum_{j=1}^{N}(U_e(j)-U_a(j))^2}{N}} \quad (7)$$

$$NRMSE = \frac{RMSE}{U_{max}-U_{min}} \quad (8)$$

$$MAE = \frac{\sum_{j=1}^{N}|U_e(j)-U_a(j)|}{N} \quad (9)$$

$$ARPE = \frac{1}{N}\sum_{j=1}^{N}\frac{|U_e(j)-U_a(j)|}{|U_a(j)|} \times 100\% \quad (10)$$

Wherein N signifies the quantity of training or testing data, $U_{max}$ represents the highest recorded value, and $U_{min}$ depicts the smallest value of the gathered data. $U_e(j)$ and $U_a(j)$ pertain to the predicted SOC yielded from the trained neural network, and the actual SOC deduced from the empirical data, respectively.

Figure 8 depicts the real and predicted SOC training outcomes for the best and worst estimated conditions using the same training data collection. For all current discharge profiles, the SOC estimate is very accurate, and the corresponding errors are close to zero, as predicted. The testing data from each test was used to determine the accuracy of the qualified ANN for SOC estimation. Figure 9 depicts a comparison of the real SOC and the predicted SOC at the temperature of 30°C for various EV discharge current profiles. To ensure the ANN's consistency, we run it 20 times at various temperatures. All estimated SOCs are found to be very similar to the corresponding real SOCs, indicating that the proposed ANN can provide reliable SOC estimation for EVs.

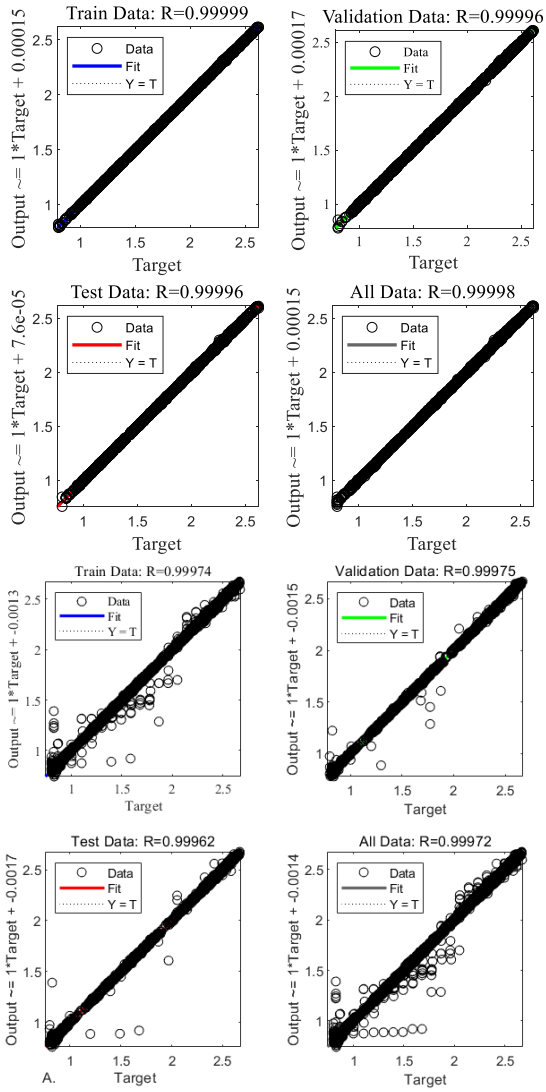


Fig. 8. Regressions of training, validation and test based outputs A. the best estimation state for JC08 driving cycle, B. the worst estimation state for ART 130 driving cycle.

TABLE 3 SOC ESTIMATION ERROR SPECIFICATIONS IN DIFFERENT CURRENT DECHARGE PROFILES OF EVS APPLICATIONS

| Driving cycle | MSE | NRMSE | ARPE | RMSE | | | MAE | | |
|---|---|---|---|---|---|---|---|---|---|
| | This Work | This Work | This Work | This Work | Others | Improvement (%) | This Work | Others | Improvement (%) |
| **WLTC** | 102e-06 | 0.0300 | 0.4393 | 0.0101 | 0.012 [14] | 19.80 | 0.00735 | 0.0085[14] | 15.65 |
| **ART 130** | 187e-06 | 0.0970 | 0.6131 | 0.0137 | | | 0.00854 | | |
| **ART Urban** | 6.2e-06 | 0.0583 | 0.1060 | 0.0025 | 0.002 [19] | -4 | 0.00178 | 0.0037[15] | 107.87 |
| **Art Rural** | 3.1e-06 | 0.0485 | 0.0737 | 0.0018 | | | 0.00120 | | |
| **WVUSUB** | 4.1e-06 | 0.0579 | 0.0897 | 0.0020 | | | 0.00147 | 0.0086[16] | 485.03 |
| **JC08** | 14e-06 | 0.0357 | 0.1710 | 0.0038 | | | 0.00279 | | |
| **JP1015** | 2.4e-06 | 0.0462 | 0.0613 | 0.0016 | 0.0064[17] | 300.00 | 0.00106 | 0.006 [17] | 475.47 |
| **NEDC** | 17e-06 | 0.0324 | 0.1679 | 0.0042 | | | 0.00280 | 0.003 [18] | 35.71 |

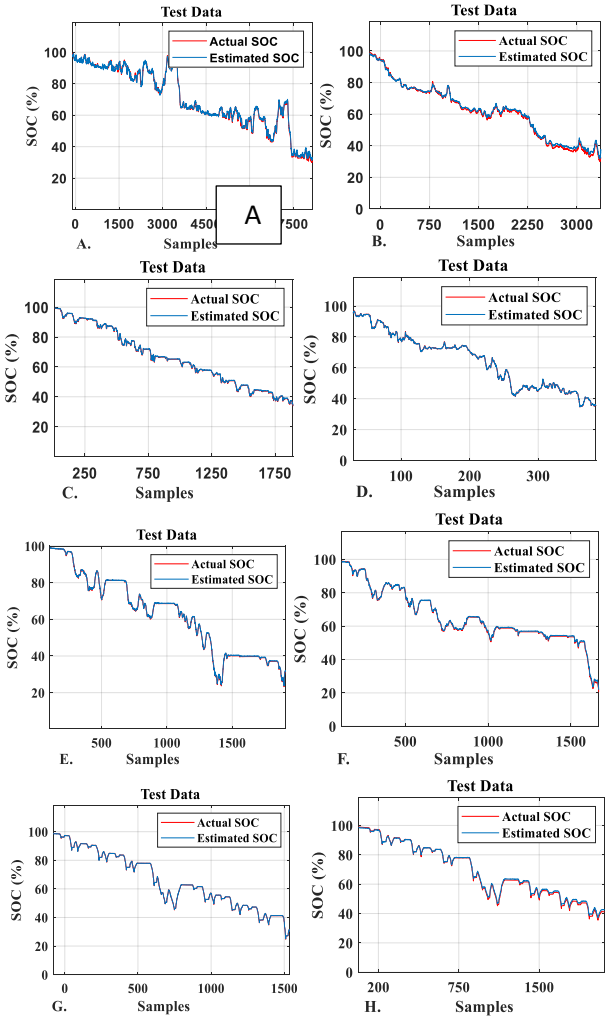


Fig. 9. Actual and estimated SOC% in different current discharge profiles, A. WLTC, B. Art 130, C. Art Urban, D. Art Rural, E. WVUSUB, F.JC08, G.JP1015, H. NEDC

Table III provides a quantitative analysis of the proposed method's robustness, presenting SOC estimation error specifications across various EV discharge current profiles. The JC08 profile yielded the smallest estimation error, while the ART 130 profile resulted in the largest. Benchmarking against existing methods demonstrates the proposed algorithm's effectiveness. Compared to the method in [14], the proposed method achieves a 19.8% reduction in RMSE and a 15.65% improvement in MAE for the WLTC profile.

While the method in [19] exhibits slightly lower RMSE for the ART Urban case, the proposed method significantly improves MAE by 107.87% compared to [15]. Furthermore, the proposed method demonstrates substantial improvements in MAE for other profiles: a 35.71% improvement for NEDC and a fivefold reduction for WVUSUB and JP1015 compared to those reported in [16] to [18], respectively.

It is worth mentioning that current ANN approach does not require the classification unit. It is another fascinating contribution of this work in comparison to other works like in [9]. The overall error of all tests for Art Rural current discharge profile is plotted in figure.10, as a typical example.

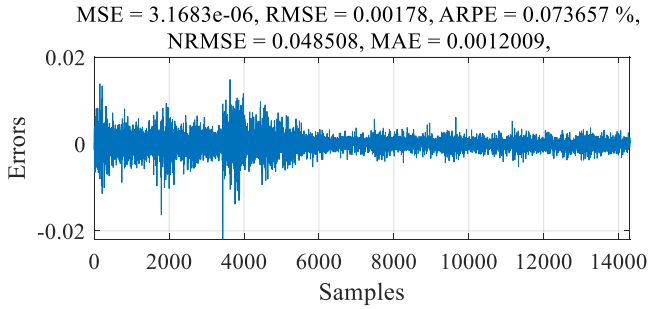


Fig. 10. Overall Errors for Art Rural current decharge profile test-set

## VI. Conclusion

This paper proposes a novel ANN approach for estimating the State-of-Charge (SOC) of supercapacitors in electric

vehicles (EVs). The key innovation lies in treating the SOC as the ANN's output and incorporating the distribution of discharged capacity as one of its inputs. This allows the ANN to capture the impact of varying discharge current profiles on the SC's residual capacity, leading to more accurate estimations tailored to different EV driving cycles.

Performance is evaluated using various error metrics (MSE, RMSE, NRMSE, ARPE, MAE) on different testing datasets. The consistently low values close to zero demonstrate the proposed three-layer ANN's capability of providing reliable SOC estimation.

Furthermore, a wavelet transform model is introduced to decompose the voltage profile into its frequency components. This information is then fused with the NN model to create a comprehensive Wavelet Neural Network (WNN) model. This combined approach significantly improves the accuracy of SOC estimation compared to the NN alone.

The WNN model demonstrates high reliability under diverse driving cycle conditions, supported by detailed error statistics. While previous work presented in [9], highlighted the lack of a classification unit for various discharge profiles, this NN approach effectively addresses this challenge. It accurately estimates the SOC of a SC module, finding potential applications in various EV scenarios.

Future work could explore extending the ANN to account for multiple SC modules and ageing effects. Despite limitations in certain hybrid EVs regarding grid-based charging and unknown fully charged states, the proposed ANN method remains applicable in such situations.

**Acknowledgment**

This research work has been supported by a research grant from the Amol University of Special Modern Technologies, Amol, Iran.

In the conclusion, please show how the work advances the field from the present state of knowledge. Please provide a clear justification for your work in this section, and indicate uses and extensions if appropriate. Moreover, you can suggest future.

## REFERENCES

[1] Lei Zhang, Zhenpo Wang, Fengchun Sun, and David G. Dorrell, “Online Parameter Identification of Ultracapacitor Models Using the Extended Kalman Filter”, Energies, Vol. 7, pp. 3204-3217, 2014.

[2] M. Jami, “Virtual Inertia Control and Small-Signal Stability Analysis of Electric Vehicle”, International Journal of Industrial Electronics, Control and Optimization (IECO), 6(4), 2023.

[3] Ramezan Havangi, Fatemeh Karimi, “Improvement of The Battery State of Charge Estimation Using Recursive Least Square Based Adaptive Extended Kalman Filter”, Industrial Electronics, Control and Optimization (IECO), 7(2), 2024.

[4] Kiarash Movassagh, Arif Raihan, Balakumar Balasingam, Krishna Pattipati, “A Critical Look at Coulomb Counting Approach for State of Charge Estimation in Batteries”, MDPI *Energies*, 14(14), 2021.

[5] Marco Mussi, Luigi Pellegrino, Marcello Restelli, Francesco Trovò, “A voltage dynamic-based state of charge estimation method for batteries storage systems”, Journal of Energy Storage, Vol. 44, Part B, 2021.

[6] Xin Zhang, Jiawei Hou, Zekun Wang, and Yueqiu Jiang, “Study of SOC Estimation by the Ampere-Hour Integral Method with Capacity Correction Based on LSTM”, MDPI *Batteries*, 8(10), 170, 2022.

[7] Jingrong Wang, Jinhao Meng, Qiao Peng, Tianqi Liu, Jichang Peng, “An electrochemical-thermal coupling model for lithium-ion battery state-of-charge estimation with improve dual particle filter framework”, Journal of Energy Storage, Vol. 87, 2024.

[8] Yoshifumi Morita, Sou Yamamoto, Sun Hee Lee, and Naoki Mizuno, “On-Line Detection Of State-Of-Charge In Lead Acid, Battery Using Radial Basis Function Neural Network”, Asian Journal of Control, Vol. 8, No. 3, pp. 268-273, 2006.

[9] W. X. Shen, K. T. Chau, C. C. Chan, and Edward W. C. Lo, “Neural Network-Based Residual Capacity Indicator for Nickel-Metal Hydride Batteries in Electric Vehicles”, IEEE transactions on vehicular technology, Vol. 54, NO. 5, pp. 1705-1712, 2005.

[10] Cheng Bo, Bai Zhifeng, Cao Binggang, “State of charge estimation based on evolutionary neural network”, Energy Conversion and Management, Vol. 49 , 2008.

[11] Juan Carlos Álvarez Antón, Paulino José García Nieto, Cecilio Blanco Viejo, José Antonio Vilán Vilán, “Support vector machines used to estimate the battery state of charge”, IEEE Trans. Power Electron. 28, 2013

[12] Simin Peng, Yifan Miao, Rui Xiong, Jiawei Bai, Mengzeng Cheng, Michael Pecht, “State of charge estimation for a parallel battery pack jointly by fuzzy-PI model regulator and adaptive unscented Kalman filter”, Applied Energy, Vol. 360, 2024.

[13] Hicham Ben Sassi, Fatima Errahimi, Najia Es-Sbai, Chakib Alaoui, “Comparative study of ANN/KF for on-board SOC estimation for vehicular applications”, Journal of Energy Storage, Vol. 25, 2019.

[14] Jie Zhang, Bo Xiao, Geng Niu, Xuanzhi Xie, Saixiang Wu, “Joint estimation of state-of-charge and state-of-power for hybrid supercapacitors using fractional-order adaptive unscented Kalman filter”, Energy, Vol. 294, 2024.

[15] Seyedmehdi Hosseininasab, Nastaran Momtaheni, Stefan Pischinger, Marco Günther, Lennart Bauer, “State-of-charge estimation of Lithium-ion batteries using an adaptive dual unscented Kalman filter based on a reduced-order model”, Journal of Energy Storage, Vol. 73, 2023.

[16] Bizhong Xia, Wenhui Zheng, Ruifeng Zhang, Zizhou Lao, and Zhen Sun, “A Novel Observer for Lithium-Ion Battery State of Charge Estimation in Electric Vehicles Based on a Second-Order Equivalent Circuit Model”, MDPI *Energies*, 2017.

[17] Yonghong Xu, Hongguang Zhang, Jian Zhang, Fubin Yang, Liang Tong, Dong Yan, Hailong Yang, Yan Wang, “State of charge estimation under different temperatures using unscented Kalman filter algorithm based on fractional-order model with multi-innovation”, Journal of Energy Storage, Vol. 56, 2022.
[18] Jinhao Meng, Daniel-Ioan Stroe, Mattia Ricco, Guangzhao Luo, and Remus Teodorescu, “A Simplified Model based State-of-Charge Estimation Approach for Lithium-ion Battery with Dynamic Linear Model”, IEEE transactions on industrial electronics, 2018.
[19] Georg Walder, Christian Campestrini, Sebastian Kohlmeier, Markus Lienkamp, Andreas Jossen, “Adaptive State and Parameter Estimation of Lithium-Ion Batteries Based on a Dual Linear Kalman Filter”, Technological Advances in Electrical, Electronics and Computer Engineering, 2014.
[20] Jonghoon Kim, Hany M. Hasanien, Roland Kobla Tagayi, “Investigation of noise suppression in experimental multi-cell battery string voltage applying various mother wavelets and decomposition levels in discrete wavelet transform for precise state-of-charge estimation”, Journal of Energy Storage, Vol. 73, Part C, 2023.
[21] Asmae El Mejdoubi, Amrane Oukaour, Hicham Chaoui, Youssef Slamani, Jalal Sabor, Hamid Gualous, “Online Supercapacitor Diagnosis for Electric Vehicle Applications”, IEEE Transactions on Vehicular Technology, Vol. 65, Issue: 6, 2016.
[22] S.S. Moosavi, A. Kazemi, H. Akbari, "A comparison of various methods of identifying open-circuit fault in the IGBT-based DC/AC inverter used in electric vehicle", Engineering Failure Analysis, Vol. 96, Pp. 223-235, 2019.
[23] S. Saeid. Moosavi, A. Djerdir, Y. A. Amirat, D. A. Khaburi, “Artificial Neural Network based Fault Detection in the AC-DC Converter of the Power Supply of SHEV”, Electrical Systems in Transportation, IET, Vol. 6, Issue 2, 2016.
[24] S. Saeid. Moosavi, A. Djerdir, Y. Aït-Amirat, D. A. Khaburi, “ANN based fault diagnosis of permanent magnet synchronous motor under stator winding shorted turn”, Electric Power Systems Research, Vol. 125, 2015.
[25] M. Sifuzzaman, M. R. Islam, M. Ali, “Application of wavelet transform and its advantages compared to fourier transform”, Journal of Physical Sciences, Vol. 13, 2009.

**Seyed Saeid Moosavi** (S’09) was born in Amol, Iran. He received the B.Sc. degree in electrical power engineering, in 2004, the M.Sc. degree from the Electrical Railway engineering department of Iran University of science and technology (IUST), Tehran, Iran, in 2009. From 2007-2010 he was a researcher on Electrification, control and signaling of railway transportation. He received the PHD in electrical engineering at university of technology Belfort Montbeliard, in 2013. He was assistant professor in the Systems and Transport (SET) laboratory at University of Technology Belfort Montbéliard, France and researcher in the FEMTO-ST laboratory in 2014. Now he is assistant professor of Amol university of special modern technologies. His main research interests include the modeling of electrical machines (EM), hybrid/electric vehicle (H/EV) and the study and application of, condition monitoring, signal processing, fault detection and diagnosis techniques for EM and H/EV.

**Mahmood Moghadasian** earned his B.S. in electronics from Amirkabir University of Technology in 2005. He then received his M.Sc. in power engineering from Shahid Chamran University of Ahvaz in 2008, and his Ph.D., also in power engineering, from UPJV, Amiens, France, in 2013. He is currently an Assistant Professor at Shohadaye Hoveizeh Campus of Technology, Shahid Chamran University of Ahvaz,. His research focuses on machine learning, optimal control, and optimization.

**Maryam Golpour** was born in Amol, Iram. She received her B.S. and M.S. degree in Chemical Engineering from the University of Guilan, Rasht, Iran, in 2009 and 2012 respectively, and her Ph.D. degrees in Chemical Engineering from the Ferdowsi University of Mashhad, Mashhad, Iran, in 2018. From 2018 until present, she is a research assistant in clean power generation and electrochemical laboratory at Amol University of Special Modern Technologies, Amol, Iran. Her current research interests include nano technology, separation, energy production, and data science.